Three-Layer Micelles of an ABC Block Copolymer: NMR, SANS, and LS Study of a Poly(2−ethylhexyl acrylate)-*block*-poly(methyl methacrylate)-*block*-poly(acrylic acid) Copolymer in D_2O

J. Kříž,* B. Masař, J. Pleštil, Z. Tuzar, H. Pospíšil, and D. Doskočilová

Institute of Macromolecular Chemistry, Academy of Sciences of the Czech Republic, Heyrovský Sq. 2, 16206 Prague 6, Czech Republic

Received June 4, 1997; Revised Manuscript Received September 25, 1997

ABSTRACT: A poly(2-ethylhexyl acrylate)-*block*-poly(methyl methacrylate)-*block*-poly(acrylic acid) (**PEHA**−**PMMA**−**PAAc**) triblock copolymer was prepared by group transfer polymerization (GTP) and subsequent acidolysis. When transferred from a molecular solution into water or D_2O, the copolymer is shown, by static light scattering (SLS) and dynamic light scattering (DLS), to form spherical micelles of a narrow size distribution. According to NMR line shape and signal intensity analysis, and SANS measurements using contrast variation by a selective swelling of **PEHA** blocks with cyclohexane-d_{12}, the three block types are mostly segregated in a micelle, **PEHA** forming the inner and **PMMA** the outer layer of the core. Both methods indicate an existence of mixed layers in which the blocks **PEHA**−**PMMA** (in the core) and **PMMA**−**PAAc** (at the outer rim of the core) are entangled. NMR data point to the temperature-dependent conflict of the influence between the **PEHA** compression resistance and the core−shell interface tension. Solvents generally penetrate more slowly into **PEHA**−**PMMA**−**PAAc** micelles than into **PMMA**−**PAAc** micelles of a comparable size, but those selective for **PEHA**, such as cyclohexane, swell the micellar core to a higher degree in the former case.

Introduction

Micelles formed by amphiphilic block copolymers in water have been the object of intensive study[1−7] both for theoretical interest and their potential applicability as surfactants or systems for controlled release of drugs or other active substances. For the latter use, there is a need for maximum solubilization capacity of the micellar core combined with a tailored permeability of the solubilizate across the core−shell interface. In our previous studies[8−11] on micelles of poly(methyl methacrylate)-*block*-poly(acrylic acid) (**PMMA**−**PAAc**) copolymers in water, we have shown that both the rate and equilibrium degree of solubilization are mostly controlled by the interaction parameter of the solubilizate with the polymer block prevalent in the core. Solubilizates with a good affinity for the core polymer are thus easily solubilized but also, as a rule, easily released from the micelle. For the potential use of polymer micelles in controlled release of some chemicals such as drugs, pesticides, and so forth, construction of systems with a high solubilization capacity of the core toward a specific class of compounds but, at the same time, a relatively high barrier against their diffusion from the core into the surrounding water and *vice versa* could be of high interest. On the basis of our earlier solubilization studies,[10,11] we expect that micelles with at least two concentric layers in their core, the outer one being formed by a quasi-glassy polymer and the inner one consisting of a much softer polymer or block with a different polarity, could have such characteristics. The important condition here is, however, that both layers are sufficiently segregated.

One of the possible solutions of this problem is that of micelles based on ABC triblock copolymers in which all three blocks are mutually incompatible, A and B being hydrophobic and C hydrophilic. As an example of such a system, we examine here poly(2-ethylhexyl acrylate)-*block*-poly(methyl methacrylate)-*block*-poly(acrylic acid) (**PEHA**−**PMMA**−**PAAc**) copolymers and micelles formed by them in water.

Experimental Section

Block Copolymers and Micellar Solutions. Poly(methyl methacrylate)-*block*-poly(acrylic acid) (**PMMA**−**PAAc**) and poly(2-ethylhexyl acrylate)-*block*-poly(acrylic acid) (**PEHA**−**PAAc**) copolymers were prepared by a successive group-transfer polymerization (GTP) of either methyl methacrylate (**MMA**) or 2-ethylhexyl acrylate (**EHA**) and *tert*-butyl acrylate (**tBuA**) and subsequent selective acidolysis of the poly(**tBuA**) block using the method described earlier.[8] In an analogous way, poly(2-ethylhexyl acrylate)-*block*-poly(methyl methacrylate)-*block*-poly(acrylic acid) (**PEHA**−**PMMA**−**PAAc**) was prepared by a successive GTP of **tBuA**, **MMA**, and **EHA** followed, after purification and characterization by size exclusion chromatography (SEC) and NMR, by selective acidolysis of the poly(**tBuA**) block. After that, the product was dissolved in a THF−water (2:1 w/w) mixture, transferred into distilled water by dialysis, and freeze-dried in the micellar form. For NMR, SANS, and LS experiments, the freeze-dried product was directly dissolved in either D_2O or distilled water.

NMR Measurements. ^{1}H NMR spectra (300.13 MHz) of mostly 0.5% w/w solutions of the block copolymers in D_2O (99.8% d) were measured with a Bruker Avance DPX 300 spectrometer using 0.01 wt % of sodium 2,2-dimethyl-2-silapentane-5-sulfonate (DSS) as internal standard. As a rule, 80 scans with selective presaturation of the remaining H_2O were done, and the exponential weighting (lb = 2 Hz) was used before Fourier transformation. T_1 and T_2 measurements were done using a conventional inversion−recovery and Carr−Purcell−Meiboom-Gill sequence with the delay between the π pulses equal to 2 ms. T_2-filtered spectra were measured with the sequence $d_1-\pi/2_x-[\tau-\pi_y-2\tau-\pi_{-y}-\tau]_n-$FID, the phases being circled according to the usual CYCLOPS scheme. With the length of the π pulse expressed in seconds, the filtering delay d_f has the value $d_f = n(2\pi + 4\tau)$. T_2-filtered$-T_1$ measurements were done with the analogous sequence, $d_1-\pi/2_x-[\tau-\pi_y-2\tau-\pi_{-y}-\tau]_n-\pi/2_x-vd-\pi/2_x-$FID, with vd being the variable delay, $\tau = 1$ ms, and $n = 20$. Selectively T_1-filtered spectra were measured with the conventional inversion−

S0024-9297(97)00800-0 CCC: $15.00
Published on Web 01/13/1998

recovery sequence, viz. $d_1-\pi_x-d_2-\pi/2_x-$FID, with $d_2 = t_1$ ln 2, t_1 being the value of T_1 obtained with the T_2-filtered$-T_1$ sequence. T_2-filtered 2D NOESY spectra were measured using the pulse sequence $d_1-\pi/2_x-[\tau-\pi_y-2\tau-\pi_{-y}-\tau]_n-\tau_0-\pi/2-\tau_m-\pi/2-$FID with $\tau = 1$ ms and $n = 20$, that is with an 80 ms T_2-filtering delay. Here, τ_0 means the incremented delay and τ_m is the mixing time (0.2 s in our case). 1024 points and 256 increments were used, taking 432 scans (60 h of measurement). Solubilization rates were observed using a stationary method with the constant boundary concentration described earlier.[10]

Small-Angle Neutron-Scattering (SANS) Measurements. SANS measurements were performed using the time-of-flight small-angle neutron spectrometer YuMO at the IBR-2 pulse reactor in the Joint Institute for Nuclear Research, Dubna.[12] The solution was placed in an optical quartz cell with a path length of 1 mm. All measurements were corrected for background scattering and normalized using a vanadium standard.[13]

The experimental SANS curves were fitted by a scattering curve for homogenous spherical particles with a two-parameter Schulz−Zimm distribution of radii. The theoretical fitting function was

$$P(q) = \int_0^\infty F(q, R)^2 f_z(R)\, dR \qquad (1)$$

where the scattering amplitude for a sphere of radius R and scattering contrast $\Delta\rho$ is

$$F(q,R) = \frac{4}{3}\pi R^3 \Delta\rho \Phi(q,R)$$

with

$$\Phi(q,R) = 3\,\frac{\sin(qR) - qR\cos(qR)}{(qR)^3}$$

The Schulz−Zimm distribution is a two-parameter function

$$f_z(R) = \left(\frac{Z+1}{R_m}\right)^{Z+1} \frac{R^Z}{\Gamma(Z+1)} \exp\left\{-\left(\frac{Z+1}{R_m}\right)R\right\}$$

where R_m is the mean radius, Z is a width parameter ($Z > -1$), and $\Gamma(x)$ is the gamma function. The fit was applied to the SANS curves taken under such contrast conditions that the scattering contribution of the micellle corona could be neglected or disregarded.

Static Light Scattering (SLS). Measurements of the molar mass of micelles were performed[14] on a Sofica instrument equipped with a He−Ne laser. Data were treated by a standard Zimm method. Refractive index increments of micelles in water (0.125 mL/g) were determined using a Brice−Phoenix differential refractometer.

Dynamic Light Scattering (DLS). The measurements were made[14] using an ALV 5000, multibit, multi-tau autocorrelator and an argon ion laser ($\lambda_0 = 514.5$ nm). Data were processed using a standard cumulant method.

Results and Discussion

The typical block copolymer **PEHA−PMMA−PAAc** studied in this paper had the average content of 31.1 units of 2-ethylhexyl acrylate (**EHA**), 56.4 units of methyl methacrylate (**MMA**), and 194.8 units of acrylic acid (**AAc**). Due to its polydispersity of molecular weights 1.43, it had the average M_w 36 358. When it was dissolved in tetrahydrofuran−water (2/1 w/w), transferred into water by stepwise dialysis, and then freeze-dried, the product was directly soluble in water or D_2O, thus forming a micellar solution. Dynamic light scattering (DLS) shows the micelles to have a fairly narrow size distribution. According to static light scattering, the M_w of the average micelle is 18×10^6; that is, the association number of the copolymer molecules in an average micelle is about 509. Compared to that, the **PMMA−PAAc** copolymer mostly studied by us in the past[8−11] had in the mean 90.2 **MMA** and 176.5 **AAc** units ($M_w/M_n = 1.21$), that is a comparable length of the hydrophobic part and a slightly shorter hydrophilic part. According to SANS, the micelles formed by the analogous procedure were considerably smaller and comprised about 200 macromolecules. In contrast to it, the **PEHA−PAAc** copolymer with 94.3 **EHA** units and 152.4 **AAc** units, that is again with a comparable length, forms much larger micelles containing about 720 macromolecules. From this, the **PEHA** block appears to cause larger association numbers. This effect could be caused by (i) the higher hydrophobicity of **PEHA** (which could be deduced for example from the much lower solubility of **EHA**, compared to **MMA**), (ii) its softness (its T_g being about 60 K below the experimental temperature), and also (iii) the higher mass contained in each **EHA** unit. Which of these factors prevails must be decided by further studies. Research in this field is far from simple, as neither the tailored synthesis of the corresponding block copolymers nor the preparation of well-defined micelles is trivial.

Chart 1

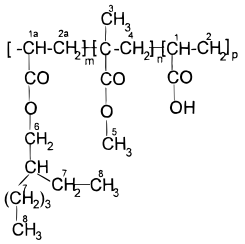

DLS gives for the freeze-dried **PEHA−PMMA−PAAc** triblock copolymer directly dissolved in pure water the value of hydrodynamic radius $r_H = 49$ nm, which expands in the borax buffer (pH 9.2) to 77 nm, showing thus the usual effect (cf. e.g. ref 9) of shell expansion in media with higher pH. The r_G value of micelles prepared by direct dissolution of the freeze-dried sample in water is 38 nm. The ratio r_H/r_G (=49/38) corresponds the value for hard spheres, $(5/3)^{1/2}$. When dissolved in THF$-H_2O$ to a molecular solution and then transferred to the borax buffer, the micelles have $r_H = 62$ nm, according to DLS. This shows that freeze-drying causes only minor micellar aggregation, and accordingly, direct dissolution of the freeze-dried polymers in D_2O can be used for NMR and SANS studies. At the same time, the difference indicates that the micelles are not quite in an equilibrium state, probably due to the quasi-glassy state of the **PMMA** part.

NMR Observation of Micellization. Throughout this paper, the protons will be designated according to Chart 1, that is with respect to our ability to discern their signals. The CH proton in the side group of **EHA** bears no number because we were unable to assign its signal (due to coupling with protons 7 and 8, it must be a broadened multiplet probably hidden by some other signal).

In contrast to the parent **PEHA−PMMA−PtBuA** copolymer, which is easily soluble in many solvents, there is only a narrow class of solvents which are able to dissolve **PEHA−PMMA−PAAc** to a molecular solution. Efficient are usually solvent mixtures containing

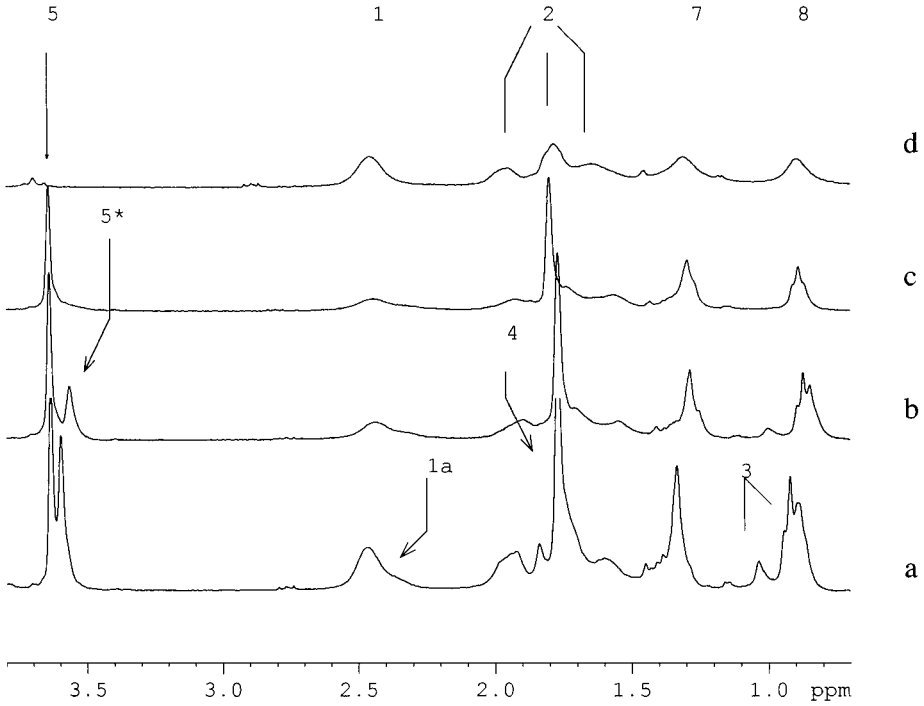

Figure 1. Relevant parts of 300.13 MHz ^{1}H NMR spectra of **PEHA**−**PMMA**−**PAAc** in THF-d_8−D_2O mixtures. D_2O content in % w/w: (a) 40, (b) 60, (c) 75, (d) 100 (330 K).

a component with medium polarity and good affinity to the **PEHA** and **PMMA** blocks (such as pyridine, dioxane, THF) and a highly polar component which dissolves **PAAc** (such as DMF and, in particular, water). The efficiency of a particular solvent mixture can be deduced from the additivity of the intensity of *all* signals in the NMR spectrum thanks to the fact that aggregation of any part of the copolymer leads to strong broadening and thus effective vanishing of the corresponding signals. In insufficiently polar media, the **PAAc** signals lose intensity due to **PAAc** aggregation and forming of reverse micelles; in highly polar (e.g. water-rich) media, **PMMA** and partly **PEHA** signals vanish due to aggregation of the corresponding blocks. This behavior of NMR spectra can be used for the study of micellization during dialysis of the solution of **PEHA**−**PMMA**−**PAAc** in THF−water solution with additional water.

Figure 1 shows relevant parts of the ^{1}H NMR spectra of **PEHA**−**PMMA**−**PAAc** in THF progressively diluted with D_2O at 330 K (the intensity of the spectrum in Figure 1d is enhanced). At this temperature and in media rich in THF, the shifting signal of the residual H_2O partly overlaps with signal 6, which is thus hidden due to presaturation. In spectra 1a and b, signals 2a cannot be clearly distinguished from signal 2 and are thus not separately assigned. There are three features of the shown development: (i) signal 5 splits into two signals, one of which decays on D_2O dilution much more rapidly than the other, (ii) the skeletal (1a, 2a) signals of the **PEHA** blocks vanish faster than those of the **PMMA** blocks whereas (iii) those of protons 7 and 8 are partly seen even in the spectra of the micellar solution of **PEHA**−**PMMA**−**PAAc** in pure D_2O at slightly elevated temperatures. The splitting of signal 5 and the behavior mentioned in (i) can be interpreted in the following way: the left sharp signal 5 has the same chemical shift as the analogous singlet in a 2:1 THF−D_2O mixture and corresponds to the molecular solution of the copolymer. The right signal, which changes its position, half width, and relative intensity on dilution of the system with water, must correspond to the emerging micellar core, which is gradually less swollen by THF. Analogous development can be observed on signal 4, where the new signal forms a shoulder in Figure 1a which is almost invisible in Figure 1b. This can be expected as the skeletal CH_2 protons become immobilized much faster than the methyl side groups. From Figure 1c, one can see that, at the ratio 1:3 (THF−D_2O), micelles with already compact cores still coexist with the dissolved unimer molecules of the copolymer. At a slightly higher D_2O content, all copolymer becomes micellized. The unequal rate of the disappearance of the skeletal signals of **PEHA** and **PMMA** mentioned in (ii) can be deduced by comparing the integral intensities of group 1 + 1a with those of group 2 + 2a + 4 and indicates that the **PEHA** block aggregates somewhat faster than the **PMMA** block; that is, **PEHA** is being incorporated into the inner part of the micellar core.

Like in the NMR spectra of micelles based on diblock copolymers,[8−11] the signals of the **PAAc** blocks are observed. Comparing their intensity in the acid and fully sodium-neutralized form or in the former and the $CHCl_3$-swollen acid form, one can deduce that about 22 mol. % of the **AAc** units in the nonswollen micellar state are in a relatively immobilized form, that is entwined or glued to the core−shell interface (cf. refs 8 and 11).

NMR Observation of the Chain Mobility in the Micellar Core. Under progressive heating of the micellar solution, signals 7 and in particular 8 increase and narrow. Figure 2 compares the proton spectra of (a) **PEHA**−**PMMA**−**PAAc** in a 0.5% w/w micellar solution, (b) bulk **PEHA**, and (c) **PEHA**−**PMMA**−**PAAc** in an approximately 7% w/w "solution", that is a hydrated gel of strongly aggregated micelles, at three different temperatures.

As one can see in Figure 1a, the signals of the micellar shell are not very affected by increasing temperature whereas those of the **PEHA** side groups 7 and 8 narrow and increase. Signal 6 of the same moiety remains hidden, and so do all skeletal **PEHA** signals and all

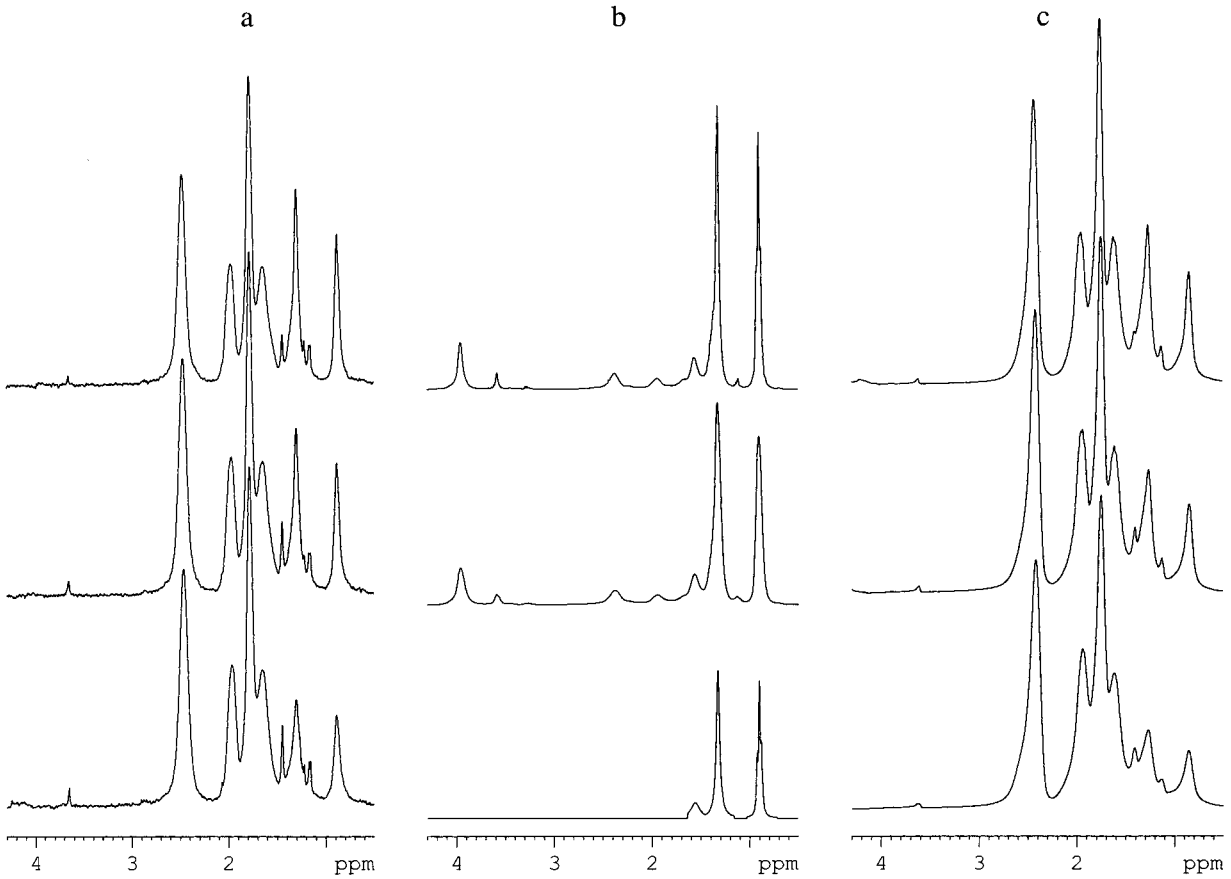

Figure 2. Relevant parts of 300.13 MHz ^{1}H NMR spectra of (a) **PEHA**−**PMMA**−**PAAc** in 0.5% solution, (b) neat **PEHA**, and (c) **PEHA**−**PMMA**−**PAAc** in ca 7% gel at (from the bottom) 333, 343, and 353 K.

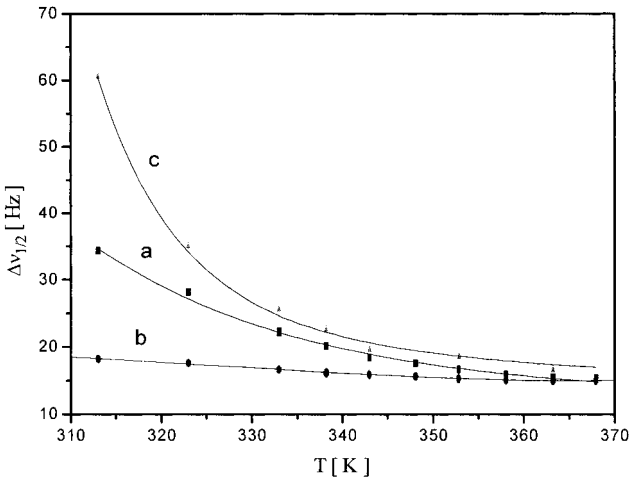

Figure 3. Temperature dependence of the signal 8 half width in 300.13 MHz ^{1}H NMR spectra of (a) **PEHA**−**PMMA**−**PAAc** in 0.5% solution, (b) neat **PEHA**, and (c) **PEHA**−**PMMA**−**PAAc** in ca. 7% gel.

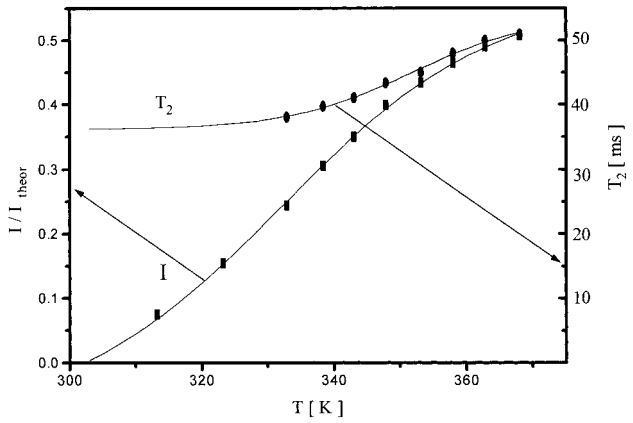

Figure 4. Relative intensity of signal 8 in 300.13 MHz ^{1}H NMR spectra of a **PEHA**−**PMMA**−**PAAc** 0.5% solution in D_2O and the corresponding value of T_2 at increasing temperature.

PMMA signals. In contrast to this case, all signals with additive intensities can be observed in bulk **PEHA** polymer (a viscous liquid) at 340 K. The spectra of the micellar gel in Figure 1c are analogous to those in Figure 1a except the signals are broader and, what is more important, of a super-Lorentzian shape.

Figure 3 shows the full temperature dependence of the signal half width of signals 8 for the three systems a−c. The steepness of the line width change increases in the order b < a < c. The half widths of signals 8 in both micellar solution and bulk **PEHA** clearly converge to a value given by *J*-splitting with the protons 7, which can also be seen from a partial resolution of the corresponding triplet above 363 K. We thus attempted to measure the T_2 values of signal 8 in the same temperature interval. Although signals 8 and 7 have very nearly a Lorentzian shape, providing their *J*-splitting is not apparent, their intensity does not decay exponentially but rather as a sum of several exponentials. Therefore, we modified our T_2 experiment evaluation by disregarding the points in the initial 30 ms, so that the experimental data were very little influenced by rapidly decaying coherences. The T_2' values acquired in such a way for system a are plotted in Figure 4 together with the corresponding intensities of the signal 8. One can see that the decrease of the transverse

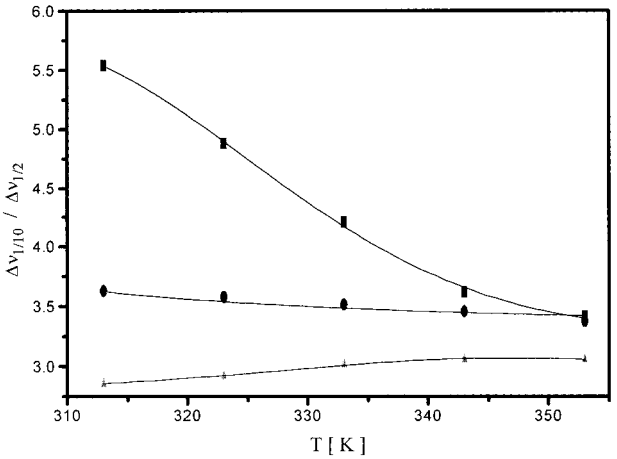

Figure 5. Temperature dependence of $\xi = \Delta\nu_{1/10}/\Delta\nu_{1/2}$ of signal 8 in 300.13 MHz ^{1}H NMR spectra of (●) **PEHA**−**PMMA**−**PAAc** in 0.5% solution, (▲) neat **PEHA**, and (■) **PEHA**−**PMMA**−**PAAc** in ca. 7% gel.

relaxation rate with increasing temperature is much less dramatic than the increase in intensity which converges, however, to approximately 50% of the theoretical value. The T_2' values measured in such an experiment thus correspond to a mere part of the protons 8, that is those with mobility sufficient to avoid excessive broadening of their signals. The same holds for protons 7, which show an even larger intensity deficit that decreases with growing temperature in a similar way. Signals 6 and those of the skeletal protons 1a and 2a are not observed at all in system a or c.

Another quite apparent feature of the temperature dependence of the spectra, in particular of the system c, is the change of signal shape. The value of $\xi = \Delta\nu_{1/10}/\Delta\nu_{1/2}$ ($\Delta_{1/j}$ being the signal width at the j-th part of its height), which is plotted against temperature in Figure 5, indicates the deviation of a signal from the theoretical Loretzian shape ($\xi = 3.0$). In the case of system a there is only slight and decreasing deviation; in system c, however, in particular at lower temperatures, there are clear signs of "super-Lorentzian" shape, that is of a convolution of a Lorentzian with a broader curve of a Lorentzian or Gaussian function.

A somewhat different spectral behavior can be observed in the case of bulk **PEHA** of P_n approximately equal to that of the corresponding blocks in the micelles (system b). Here, all signals can be observed at temperatures above 313 K with additive intensities, the signal shape of protons 8 changing from Gaussian to Lorentzian shape between 313 and 323 K. In the interval from 293 to 313 K, the signals 7 and 8 are still observable but the others are broadened almost beyond detection.

Comparing spectra of systems a and b, we can see that the system of **PEHA** blocks does not behave like a microscopic droplet of bulk **PEHA** polymer. The difference is even more striking when comparing systems b and c. In considering such a difference, one has to bear in mind that bulk **PEHA** (system b) is a highly viscous liquid well above its glass transition in the whole range of our observation, which allows a nearly isotropic motion with correlation time short enough to suppress most of the dipolar broadening. In a micelle (i.e. system a or c), **PEHA** blocks are always anchored to the **PMMA** layer, which is below its T_g in the whole range of observation, and thus always restricted in their motion, relative to that of the whole micelle, on one of their ends. Some part of them, however, should have local motional freedom comparable to that of the bulk polymer. Comparing systems a and b, one can see that this evidently is not so: part of the signals of even the side groups is broadened beyond detection, and the visible part has line widths larger than the corresponding signals in the bulk hompolymer. Comparison of systems a and c shows that free tumbling of the whole micelle affects both the width and shape of these signals.

To understand these effects, one has to bear in mind (cf. refs 15−18) that mobility constraints of the polymer chains can affect the shape of NMR signals in two slightly different ways: (i) local immobilization leads to a near-static dipolar broadening which can make the signal undetectable by high-resolution NMR; (ii) more distant constraints limiting the attainable angle between the internuclear vectors and the vector of the main magnetic field lead to an additional broadening component, giving the signal a super-Lorentzian shape. Thermally activated local motion can affect (i), that is narrow NMR signals to a degree depending on its correlation time and the degree to which it is spatially isotropic. In addition to this, collective motion (either isotropic tumbling or magic angle rotation) of the sample or its decisive part (such as the whole micelle) can further narrow the signal, providing (cf. refs 16−18) its frequency is comparable to the local static dipolar broadening, and remove (ii), the super-Lorentzian additional broadening.

To appreciate the effect of micellar tumbling, we take the typical value of the hydrodynamic radius of the whole micelle (corresponding to the outer spherical profile of its shell), $r_H = 4.9 \times 10^{-6}$ cm, from dynamic light scattering. Using the Debye expression for the rotational diffusion correlation time $\tau_c = 4\pi r_H^3\eta/3kT$ (where η is the viscosity of the medium in the vicinity of the outer profile of the micellar shell and k is the Boltzmann constant), we obtain, for example for pure water and 333 K, the value $\tau_c = 5.027 \times 10^{-5}$ s. In other words, the thermal rotation of the micelles has a frequency of about 3 kHz. The tumbling of the micelle could thus cooperate with the more rapid but possibly anisotropic local motions in canceling the residual dipolar line broadening of protons 7 and 8. Such an effect of the tumbling of the whole micelle on the signal narrowing was suggested in the case of double-layer reverse micelles in organic media.[19] As the frequency in our case ∼3 kHz is one order of magnitude lower than the usual dipolar broadening in glassy polymers (40−60 kHz), such an effect can be expected with the **PEHA** blocks (in particular the ends of their side groups, i.e. protons 7 and 8) sufficiently segregated from **PMMA**.

Comparing systems a and c, in particular the temperature dependences of ξ, one can see that micellar free tumbling affects not only the line width but even more strongly the line shape of the corresponding NMR signals. This can be explained as follows. Each **PEHA** block is chemically anchored by its one end to the quasi-glassy **PMMA**; that is, this one end can be seen as fixed in a coordinate frame moving with the whole micelle. The individual monomer units of **PEHA** along with their side groups are thus restrained in their motion in dependence on their proximity to the anchor. It can be expected that, for a substantial part of them, spatially isotropic motion is prevented to some degree. In such a case and under relatively mild approximations (cf. ref

20), the line shape can be expressed as a convolution of two functions

$$I(\omega) = \int_{-\infty}^{\infty} Q_1(\omega-\omega_1)\, Q_2(\omega_1-\omega_0)\, \mathrm{d}\omega_1 \qquad (2)$$

where

$$Q_i(\omega) = \int_{-\infty}^{\infty} \exp(-i\omega t)\, \exp[-\omega_{2i}{}^2 \int_0^t (t-\tau) \times \exp(-|\tau|/\tau_i)\, \mathrm{d}\tau]\, \mathrm{d}t \qquad (3)$$

$\omega_{2i}{}^2$ and τ_i being the second moment and the respective correlation time of the "narrow" ($i = 1$, Lorentzian if $\omega_{21}{}^2\tau_1 \ll 1$) and dipolar broadening ($i = 2$, probably Gaussian) component. The result is a "super-Lorentzian" (cf. ref 20) shape ($\xi > 3$).

From the point of view of NMR, the concept of "fixing" or rather spatial constraint of the internuclear vectors is merely relative to a certain time window, however. Effectively, the monomer units and their side groups near to the **PMMA** anchor will always be constrained whereas other units, farther removed from the chemical or physical constraints, can be relatively free. Under such a situation, the signal of protons 8 can be expected to be a superposition of many slightly different line-shape functions varying from a Lorentzian to a pronounced "super-Lorentzian" shape. Considering this, eq 3 can be generalized (cf. ref 21) for the broadening component

$$Q_2(\omega) = \int_{-\infty}^{\infty} \exp(-i\omega t)\, \exp[-\sum_{j=1}^{n} w_j\, \omega_{2j}{}^2 \int_0^t (t-\tau) \times \exp(-|\tau|/\tau_{2j})\, \mathrm{d}\tau]\, \mathrm{d}t \qquad (4)$$

where w_j, $\omega_{2j}{}^2$, and τ_{2j} are the distribution weight, the second moment, and the corresponding correlation time of the j-th component. Both w_j and τ_j depend on the mobility of the "fixed" points. It can be shown,[21] for example for $w(\omega_{2j}{}^2)$ being a simple χ^2 distribution, that even relative immobilization of the ends of the blocks should lead to "super-Lorentzian" line shape with moderate values of ξ, such as observed in our case.

When the motional constraints exerted by micellar aggregation in system c are increasingly overcome by thermal activation and the micellar tumbling is thus accelerated, the dipolar broadening component is narrowed and the line shape approaches the Lorentzian one at higher temperatures, as observed.

Simulations based on eq 4 indicate that, for about 20−30 mol % of the **PEHA** monomer units in the micellar core, spatially isotropic movement should be attainable at 333 K independently of the movement of the micelle as a whole. This is proved in the following experiments. When the NMR spectrum of system c is obtained using a T_2-filter (i.e. the FIDs are accumulated with an appropriate delay d_f after the flipping pulse), the components of the signals rapidly decaying due to fast transverse relaxation practically vanish. In such a case, the spectrum contains mostly signals corresponding to groups having a relatively fast and nearly isotropic motion. In our case, this is achieved, for example, with $d_f = 80$ ms at 333 K for signals 8. The line shape of these "purified" signals is purely Lorentzian; their half width is about the same as that of the analogous signals in the system a. Their intensity, after correction for relaxation during d_f, is about 18% of the "crude" (original) signal. In contrast to the case for the bulk **PEHA**, this is the approximate fraction of the groups 8 in the inner core which have sufficient motional freedom to go through all possible angles with the vector of the magnetic field.

To find out if the "super-Lorentzian" shape of the "crude" signal 8 in system c is not simply due to a superposition of two overlapping Lorentzian signals with different widths, corresponding to two kinds of proton 8 with different motional behavior, we performed the following steps. We measured the T_2-filtered T_1 of the "purified" signal 8, obtaining the value 0.34 s. After that, we measured spectra using the T_1 filter with the d_2 value such as to null the "purified" signal in the accumulated FID. The result was a signal of very nearly the same shape as that of the original "crude" signal. This shows that most of the "super-Lorentzian" shape of 8 in the ordinary spectra of system c is really caused by residual near-static dipolar interactions due to lateral motional restriction of **PEHA** blocks. As the difference in D_2O content between systems c and a cannot have an important influence on the state of the inner core, the same relative restriction must be operative in system a, but its effect is canceled by the free tumbling of the whole micelle.

Returning now to system a, the near-Lorentzian shape of the observable part of signal 8 at all temperatures (except the highest ones, where the emerging triplet splitting of the signal distorts the shape) suggests that the relevant fraction of methyl groups is able to move in a nearly isotropic way. However, the intensity deficit markedly decreasing with growing temperature shows that a part of protons 8 remains in a state in which both methyl rotation and thermal tumbling of the whole micelle cannot effectively cancel the static dipolar broadening. From this, we see that the **PEHA** blocks in the inner core of a micelle are in a state of motional freedom definitely lower than that of the segments of bulk **PEHA**. The temperature dependence of the observable fraction of groups 8 in system a, which fits well to a Boltzmann sigmoidal distribution function, suggests the existence of an energy barrier of about 32 kJ/mol which has to be crossed by the group for it to be observed. The perceptibly steeper temperature dependence of the signal width in comparison with that of bulk **PEHA** in Figure 3 shows larger constraints to the relevant motion. The conclusion can thus be made that a considerable part of the **PEHA** blocks in the micelle has a perceptibly lower mobility than **PEHA** chains in bulk homopolymer.

The different mobilities of the **PEHA** and **PMMA** groups shown in the previous section indicate but do not really prove segregation of the corresponding blocks in the micellar core. Much more convincing arguments in this direction can be obtained from solubilization experiments using NMR or SANS techniques which are reported in the two subsequent sections.

Solubilization Observed by NMR. Figure 6 shows the development of the observable parts of the ^1H NMR spectra of **PEHA**−**PMMA**−**PAAc** under diffusion of cyclohexane through the surrounding water into the micellar core; Figure 7 gives the corresponding solubilization curve in comparison with that measured with **PMMA**−**PAAc** and **PEHA**−**PAAc** micelles of comparable size. In the spectra, the symbol 2a points to the separately visible part of the whole resonance of the corresponding protons, the remaining part being hidden by the signals 2. In the development of the spectra,

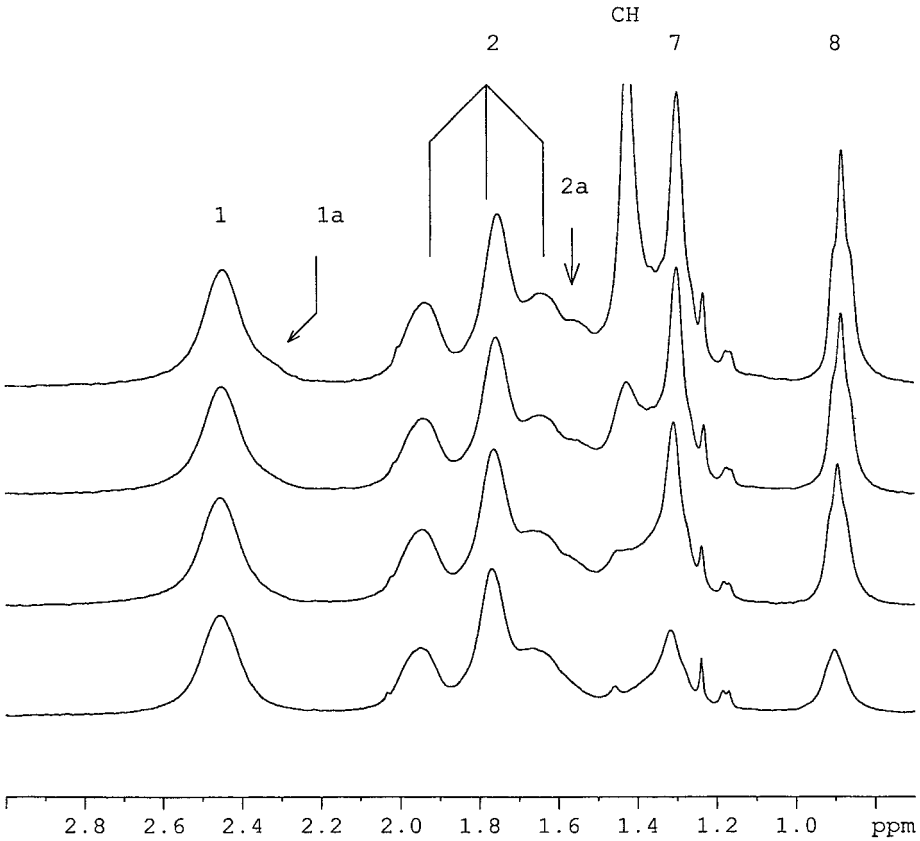

Figure 6. 300.13 MHz ^{1}H NMR spectra of **PEHA−PMMA−PAAc** in D_2O at 330 K under solubilization of cyclohexane (signal CH) after (starting from the bottom) 12, 24, 48, and 60 h.

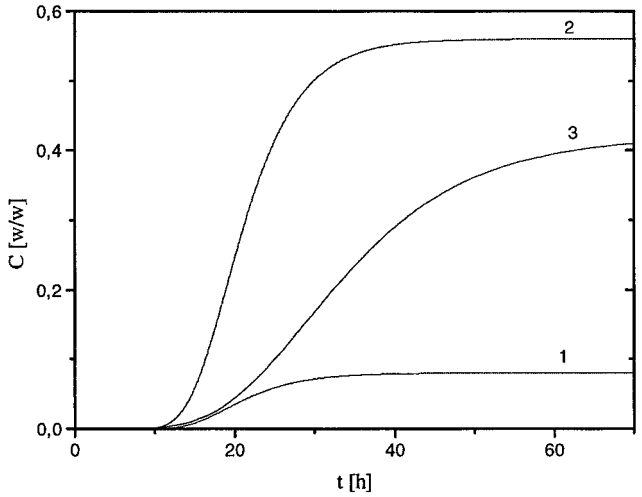

Figure 7. Time dependences of the solubilized weight of cyclohexane relative to the weight of the micellar core in (1) **PMMA−PAAc**, (2) **PEHA−PAAc**, and (3) **PEHA−PMMA−PAAc** micelles (micellar concentration 0.5 wt % in D_2O, 330 K).

there are two remarkable features: (i) in the course of cyclohexane swelling of the core, signals 7 and in particular 8 narrow and increase in the same way as they do with increasing temperature, and (ii) the only signals which are newly revealed at higher swelling degrees are those of the **PEHA** skeletal protons but none of the **PMMA** part of the micellar core. Comparison of the corresponding solubilization curves of cyclohexane (**CH**) for **PEHA−PMMA−PAAc**, **PMMA−PAAc**, and **PEHA−PAAc** in Figure 7 shows that the **PMMA** and **PEHA** parts in the **PEHA−PMMA−PAAc** core take up almost the same relative amounts of **CH** as the corresponding cores in the diblock micelles, the swelling capacity of **PMMA** being substantially lower than that of **PEHA**. As **CH** is a very poor solvent for **PMMA**, this is only to be expected for **PMMA−PAAc**. In **PEHA−PMMA−PAAc**, however, such a result is possible only if the **PMMA** blocks are mostly segregated from those of **PEHA**.

The solubilization curves in Figure 7 also show that the permeability of the core−shell interface to **CH** is approximately equal in **PEHA−PMMA−PAAc** and **PMMA−PAAc** micelles but that the solubilization capacity for this solvent is distinctly higher in the former case. Hence the possibility of tailoring a desired combination of solubilization capacity and uptake/release rate for a specific solubilizate using a multilayered micellar core is demonstrated.

As an example of the core swelling by a *nonselective* solvent, Figure 8 shows relevant parts of the NMR spectra measured in the early stages of chloroform solubilization. As expected for the radially segregated **PMMA** and **PEHA** blocks, the characteristic signals of **PMMA** emerge somewhat faster than those of **PEHA**. It is remarkable, however, that even in the quite early stages of core swelling, where only first traces of **PMMA** signals emerge, the 7 and 8 signals of **PEHA** already start increasing and narrowing, the width-to-intensity ratio following approximately the same curve as in the above-reported temperature dependence. There are two different reasons imaginable: (a) disentwining of **PMMA** and **PEHA** segments in the mixed layer and (b) interplay between the individual micellar layers and their interfaces.

(a) Even a slight loosening of motional constraints of the anchoring **PEHA** segments can lead to a substantial

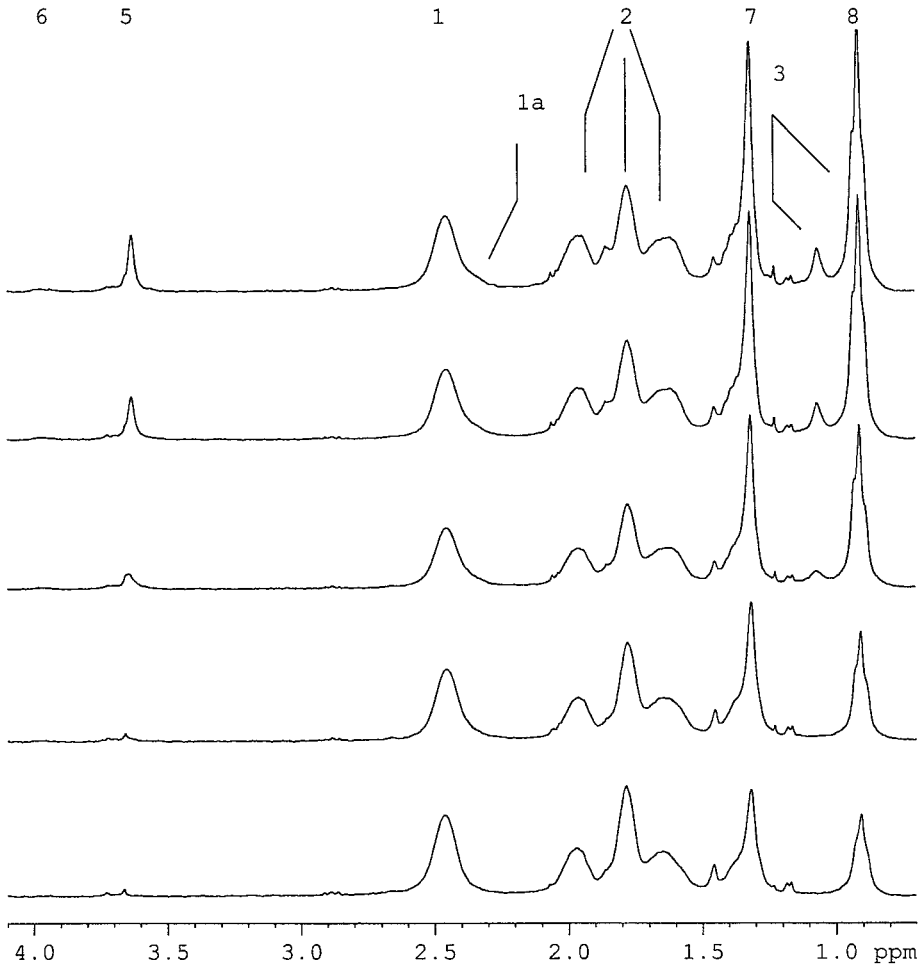

Figure 8. Relevant parts of 300.13 MHz ^{1}H NMR spectra of **PEHA**−**PMMA**−**PAAc** in D_2O under solubilization of chloroform after (starting from the bottom) 6, 12, 18, 24, 30, and 36 h at 330 K.

decrease in the anisotropy of motion (and the resulting signal narrowing) of the attached units. In particular, even partial disentangling of the incompletely segregated **PEHA** segments could affect it strongly. However, the early onset of the signal enhancement, corresponding with the swelling of the outermost surface of the **PMMA** layer, appears to exclude this process from being the main reason for the observed effect.

(b) During formation of a micelle via dialysis, several competing phenomena may be operative: (i) the **PMMA**−hydrated **PAAc** interphase tension, (ii) the adverse or segregating force between the **PMMA** and **PEHA** blocks due to their incompatibility, (iii) the resistance of **PEHA** blocks against their squeezing, and (iv) the cohesion of **PMMA** blocks and their freezing into a quasi-glassy state. Effects i and ii compete with effect iii and should be balanced in equilibrium. There is some evidence (cf. refs 6 and 7) that slightly nonequilibrium states are formed even during careful dialysis due to effect iv, but this cannot be the main explanation because the described phenomena are reversible, albeit with some hysteresis. Our results point to the conclusion that, in a micelle, the **PEHA** segments are forced into an unusually constrained state in which their mobility is restricted. When the core relaxes either by thermal activation or swelling, the PEHA segments probably attain their natural configuration and, in consequence, their natural mobility.

Most of our results reported so far pointed to segregation between the **PEHA**, **PMMA**, and **PAAc** blocks in a micelle. From the point of view of thermodynamics, however, complete segregation is not very probable. Like in the case of **PMMA**−**PAAc** diblock micelles,[8,10] we detected an about 22% increase in the integral intensity of the **PAAc** signals during chloroform solubilization, which should be due to an escape of the corresponding parts of these blocks which were mixed with parts of the **PMMA** blocks. Similarly, a partial mixing of **PMMA** and **PEHA** blocks should be probable and could be indicated by the above-mentioned splitting of the 5 signal during dilution of the molecular solution in THF with water. It is, however, very difficult to prove, and the following experiment can serve as a mere indication of its existence.

The easiest way to prove the statistical vicinty of two different groups is the existence of a nonvanishing nuclear Overhauser effect (NOE) between them. In our case, the incident groups of entangled **PMMA** and **PEHA** groups can be observed only under swelling the core with chloroform. Under such conditions, however, signals 3 and 8 overlap, so that a NOESY crosspeak between signals 5 and 8 cannot be distiguished from that between signals 5 and 3, the latter being a trivial consequence of structure. To overcome this difficulty, we designed a T_2-filtered variant of NOESY described in the Experimental Section in which the evolution of chemical shifts is preceded by a T_2-filtering sequence so that no fast relaxing components are involved in the 2D spectrum. Using model experiments with **PMMA**−**PAAc** micelles swollen with chloroform, we have found

that a 80-ms duration of this sequence is long enough to filter off any 3 or 2 resonance. Applying thus this duration in the T_2-filtered NOESY of the present system, we obtained, after 60 h of measurement, a very faint crosspeak between the remaining signals 5 and 7 and an even weaker one between signals 5 and 8, which should be an indication of a partial mixing between the **PEHA** and **PMMA** blocks.

SANS Results. The NMR results indicate segregation of the **PEHA** and **PMMA** blocks in a micelle. There are two possible structures compatible with this finding: (a) The **PEHA** blocks form an inner core surrounded by the **PMMA** layer (three-layer model); (b) The **PEHA** blocks are located in several smaller domains in a **PMMA** matrix (multidomain model). In principle, SANS can discriminate between these two models by measuring the size of the whole micellar core (formed by **PMMA** and **PEHA**) and of its **PEHA** constituent. For the three-layer model, the radius of the **PEHA** component, R_A, would be smaller than the overall radius of the micelle core, R_{AB}, while for the multidomain model the radii are expected to be very close to each other.

The neutron-scattering densities were calculated to be $\rho_A = 0.3 \times 10^{10}$ cm^{-2} and $\rho_B = 1.1 \times 10^{10}$ cm^{-2} for **PEHA** and **PMMA**, respectively. This difference in scattering densities enables one to suppress the scattering contribution of one of the components while keeping scattering from the other component still visible. The scattering density of the third component, **PAAc**, depends on the degree of neutralization and on the H/D ratio in the H_2O/D_2O mixture. Using the partial molar volume of **PAAc**,[22] $\bar{V} = 46.7$ cm^3/mol, and its change upon neutralization,[24] $\Delta\bar{V} = -14.6$ cm^3/mol, we estimated the scattering densities of the H_2O/D_2O mixture matching those of **PAAc** to be $\rho_0 = 2.8 \times 10^{10}$ cm^{-2} and $\rho_0 = 3.8 \times 10^{10}$ cm^{-2} for the acid and fully ionized forms, respectively. The contribution of condensed Na counterions was not taken into consideration in the latter quantity.

The micelle comprising the ABC triblock copolymer is a three-component particle with constituents differing in scattering density. Therefore, when the scattering density of the solvent is chosen to match the scattering density of one of the blocks, there still remain two types of blocks contributing to the scattering. This circumstance complicates interpretation of the SANS curves. Fortunately, in some cases the influence of the second not-matched component is either small or limited to a certain part of the scattering curve and the structural parameters related to the investigated component can be estimated.

In this work we attempted to distinguish between the two above given models by measuring the radii R_A and R_{AB}. To this end we used the SANS curves taken for the aqueous solvents with the scattering densities matching those of **PMMA** and **PAAc**. The corresponding radii were determined using the formulas valid for homogeneous spheres (eq 1). For the above-mentioned reason, this approach is only an approximate way to determine the structural characteristics of three-component particles. Justification of this procedure for the system under study will be examined by the calculation of theoretical scattering curves based on simple structure models (coated sphere, Gaussian chains attached to spherical core).

Figure 9 shows the SANS curves of the micellar solutions in the H_2O/D_2O mixtures matching the scattering density of the **PAAc** corona (upper curves) or that of **PMMA** chains in the core (bottom curves). The solid lines are least-square fits by eq 1.

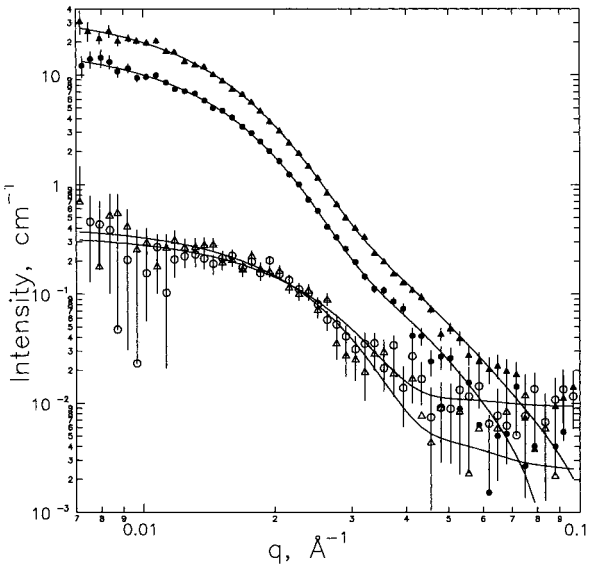

Figure 9. Experimental SANS curves (points with error bars) for the **PEHA**−**PMMA**−**PMMA** micelles in H_2O−D_2O mixtures for acid (○, ●) and sodium-neutralized **PMMA** (△, ▲). Copolymer concentration $c = 0.004\,65$ g/mL. Upper curves: zero contrast of the **PAAc** corona (acid form, 49% D_2O (●); neutralized form, 63% D_2O (△)). Bottom curves: zero contrast for **PMMA** (24% D_2O, acid form (●), neutralized form (▲)). Solid lines are least-square fits to eq 1.

The fits of the curves recorded at zero contrast for the **PAAc** chains lead to the mean core radii $R_{AB} = 120(2)$ Å for the acid form and $R_{AB} = 117(2)$ Å for fully neutralized **PAAc**. A good agreement of these results obtained at different scattering contrasts suggests that the two-component nature of the micelle core does not influence dramatically scattering behavior at these contrasts.

The SANS curves obtained for the matched **PMMA** scattering density (24% D_2O) do not show any significant difference between the results for acid and neutralized **PAAc**. This indicates that the scattering contribution of the **PAAc** corona is not too large, because the two states examined differ in scattering power. Therefore, the SANS curves reflect mainly the structure of the **PEHA** component. From the fit to eq 1 we obtained $R_A = 89(10)$ Å and $R_A = 91(10)$ Å for the sample with acid and sodium-neutralized **PAAc** corona, respectively. Low scattering intensities of the SANS (see Figure 10) data lead to great uncertainty in the values of the fitting parameters. Nevertheless, the mean radius of the **PEHA** component, R_A, seems to be significantly smaller than the overall radius of the micelle core, R_{AB}. Thus the SANS results point to the three-layer model rather than the multidomain one.

In the determination of R_{AB} we neglected the difference in the scattering densities of **PMMA** and **PEHA**. Similarly, the radius R_A was estimated using the assumption that the relevant part of the SANS curve is not affected by the scattering from the **PAAc** corona. To assess the influence of these approximations on the resulting radii, we calculated scattering curves of a coated sphere and of a micelle model with Gaussian chains attached to a spherical core. The latter model was recently proposed by Pedersen and Gerstenberg.[24]

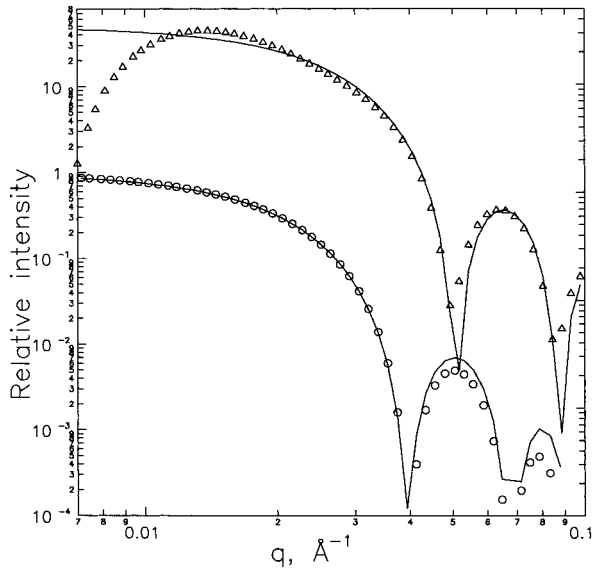

Figure 10. Illustration of the influence of the approximations made in the interpretation of the SANS data of the ABC micelles. Theoretical scattering curves for a coated sphere (○) and for a micelle model with Gaussian chains attached to the spherical core[20] (Δ). Solid lines are fits to eq 1 (homogeneous spheres). Model parameteres were chosen to be appropriate for the studied ABC micelles under corresponding contrast conditions. See the text for the model and fitting parameters.

The model parameters were chosen so as to describe the studied ABC micelles at the particular contrast conditions: For the coated-sphere model the relevant parameters were the radii R_1 (90 Å) and R_2 (120 Å) and the excess scattering amplitude fraction of the core, $\Delta b_{core}/\Delta b_{total}$, (0.518). The following parameters were used for the Pedersen and Gerstenberg model: aggregation number, $N_{agg} = 500$ Å; sphere radius, $R = 90$ Å; radius of gyration of the chain (estimated using the hydrodynamic radius of the micelle, $R_H = 490$ Å), $R_g = 150$ Å; the relative excess scattering amplitudes of the copolymer blocks were $\Delta b_{core} = -1$ and $\Delta b_{chain} = 2.74$; the chains were assumed to start at the distance $R_{start} = R_{AB} + R_g = 270$ Å from the micelle center. The last parameter mimics the effect of nonpenetration of the chains into the core.

The calculated curves were analyzed using eq 1, which is valid for homogeneous spheres. Figure 10 shows that the model curves can be fitted to the theoretical functions for homogeneous spheres quite well in most parts of the q-range probed in this experiment. This fit results in the radius $R = 114$ Å, which is about 5% lower than the true radius of the coated sphere. Therefore, the determined values of R_{AB} are slightly underestimated.

The influence of the unmatched corona is apparent at the smallest q's. Disregarding this part of the scattering curve leads to the mean radius $R = 88.3$ Å, which is very close to the true value (90 Å). Thus the procedures used could provide an acceptable approximation to the micellar radii R_A and R_{AB}.

Analysis of the SANS data provided also the mean volumes of the **PEHA**−**PMMA** core, $V_{AB} = 15 \times 10^6 \times$ Å^3, and of its **PEHA** constituent, $V_A = 4.5 \times 10^6 \times$ Å^3. These mean volumes were calculated using the distribution parameters R_m and Z and correspond to the average volume provided by scattering experiments , $\langle V^2\rangle/\langle V\rangle$, where the brackets denote number average. Micellar mass was calculated as $M_w = VN_A d/w$, where d and w are the density and mass fraction of the core, respectively, and N_A is Avogadro's number. Utilizing the mass fractions of **PEHA** (0.226) and **PEHA** + **PMMA** (0.448), we obtained the micellar masses $M_w^{AB} = 22 \times 10^6$ g/mol and $M_w^A = 12 \times 10^6$ g/mol. The value calculated from the overall core volume V_{AB} is in a good agreement with the LS result. The value obtained from the **PEHA** core is significantly lower. This may be due to the existence of a layer with intermingled **PEHA** and **PMMA** chains, indicated by the NMR results.

In ref 8 we reported some parameters of the micelles formed by the **PMMA**−**PAAc** diblock copolymer with the masses of the blocks very close to those of the hydrophobic (**PEHA** + **PMMA**) and hydrophilic (**PAAc**) parts, respectively, of the triblock copolymer used in the present study. The core radius, $R_c = 68$ Å, and the molar mass, $M_w = 3.9 \times 10^6$ g/mol, of the diblock copolymer micelles were much lower than the respective parameters of the ABC triblock copolymer. Direct comparison of these results, however, may be confusing because though both micelles were studied in aqueous media, they were originally prepared in different solvents.

Conclusions

Combining the results of our NMR, SANS, SLS, and DLS measurements, we can conclude that (i) the **PEHA**−**PMMA**−**PAAc** triblock copolymer under investigation forms in water or D_2O approximately spherical micelles with a narrow size distribution, the **PAAc** (or **PAAcNa**, **PAAcLi**) blocks forming the micellar shell more or less interpenetrating with the surrounding water; (ii) the **PEHA** and **PMMA** blocks are placed in the micellar core in a mostly segregated state, the **PEHA** blocks forming the inner core and the **PMMA** blocks located in the outer part of the core; (iii) on the interfaces between the micellar shell and the core rim and between the outer- and inner-core layers there are zones containing interwoven segments of the corresponding blocks; (iv) in the temperature range between 293 and 363 K, the **PMMA** blocks in the outer-core layer are in a quasi-glassy state whereas the inner-core **PEHA** blocks are in a state of temperature-dependent mobility which is always more constrained than that in bulk **PEHA** of a comparable molecular weight; (v) due to thermodynamic relations in the core, the uptake of low-molecular-weight substances by the **PEHA**−**PMMA**−**PAAc** micelles is generally slower than that by comparable **PMMA**−**PAAc** micelles; and (vi) however, the uptake capacity for solvents good for **PEHA** and poor for **PMMA** such as hexane, heptane, or cyclohexane is markedly larger in the case of **PEHA**−**PMMA**−**PAAc** micelles, though limited by the resistance of the **PMMA** core rim.

Acknowledgment. The authors thank the Grant Agency of the Czech Republic for its financial support given under the grants 203/95/1319, 203/93/1057, 203/96/1381, and 203/96/1387.

References and Notes

(1) Tuzar, Z.; Webber, S. E.; Ramireddy, C.; Munk, P. *Polym. Prepr. (Am. Chem. Soc., Div. Polym. Chem.)* **1991**, *32* (1), 525.
(2) Hurter, P. N.; Hatton, T. A. *Langmuir* **1992**, *8*, 1291.
(3) Kiserow, D.; Procházka, K.; Ramireddy, C.; Tuzar, Z.; Munk, P.; Webber, S. E. *Macromolecules* **1992**, *25*, 4613.
(4) Zhang, L.; Eisenberg, A. *Science* **1995**, *268*, 1728.
(5) Chu, B. *Langmuir* **1995**, *11*, 414.

(6) Moffit, M.; Zhang, L.; Khongaz, K.; Eisenberg, A. In *Solvents and Selforganization of Polymers*; Webber, S. E., Munk, P., Tuzar, Z., Eds. Kluwer Academic Publishers: Dodrecht, 1996; p 53.
(7) Almgren, M.; Brown, W.; Hvidt, S. *Colloid. Polym. Sci.* **1995**, *273*, 2.
(8) Kříž, J.; Masař, B.; Pospíšil, H.; Pleštil, J.; Tuzar, Z.; Kiselev, M. A. *Macromolecules* **1996**, *29*, 7853.
(9) Kříž, J.; Masař, B.; Dybal, J.; Doskočilová, D. *Macromolecules* **1997**, *30*, 3302.
(10) Kříž, J.; Masař, B.; Doskočilová, D. *Macromolecules* **1997**, *30*, 4391.
(11) Kříž, J.; Masař, B.; Dybal, J. *Macromolecules*, submitted.
(12) Ostanevich, Yu. M. *Makromol. Chem., Macromol. Symp.* **1988**, *15*, 91.
(13) Pleštil, J.; Ostanevich, Yu. M.; Bezzabotnov, V. Yu.; Hlavatá, D. *Polymer* **1986**, *27*, 1241.
(14) Tuzar, Z.; Pospíšil, H.; Pleštil, J.; Lowe, A. B.; Baines, F. L.; Billingham, N. C.; Armes, S. P. *Macromolecules* **1997**, *30*, 2509.
(15) Gutowsky, H. S.; Pake, G. E. *J. Chem. Phys.* **1950**, *18*, 162.
(16) Andrew, E. R.; Jasinski, A. *Solid State Phys.* **1971**, *4*, 391.
(17) Schneider, B.; Pivcová, H.; Doskočilová, D. *Macromolecules* **1972**, *5*, 120.
(18) Doskočilová, D.; Schneider, B. *Adv. Colloid Interface Sci.* **1978**, *9*, 63.
(19) Spěváček, J. *Makromol. Chem., Rapid Commun.* **1982**, *3*, 697.
(20) Doskočilová, D.; Schneider, B. *Pure Appl.Chem.* **1982**, *54*, 575.
(21) Jakeš, J. *Collect. Czech. Chem. Commun.* **1983**, *48*, 2028.
(22) Tondre, C.; Zana, R. *J. Phys. Chem.* **1972**, *76*, 3451.
(23) Ikegami, A. *Biopolymers* **1968**, *6*, 431.
(24) Pedersen, J. S.; Gerstenberg, M. C. *Macromolecules* **1996**, *29*, 1363.

MA9708003